Expression levels of GATA1s isoform affect megakaryocyte differentiation and leukemic predisposition in mice

Daishi Ishihara, Atsushi Hasegawa, Ikuo Hirano, James Douglas Engel,
Masayuki Yamamoto and Ritsuko Shimizu

List of Supporting Information

Supplementary Fig. 1

Increase of megakaryocytes in ΔNTR-H and ΔNTR-M embryos

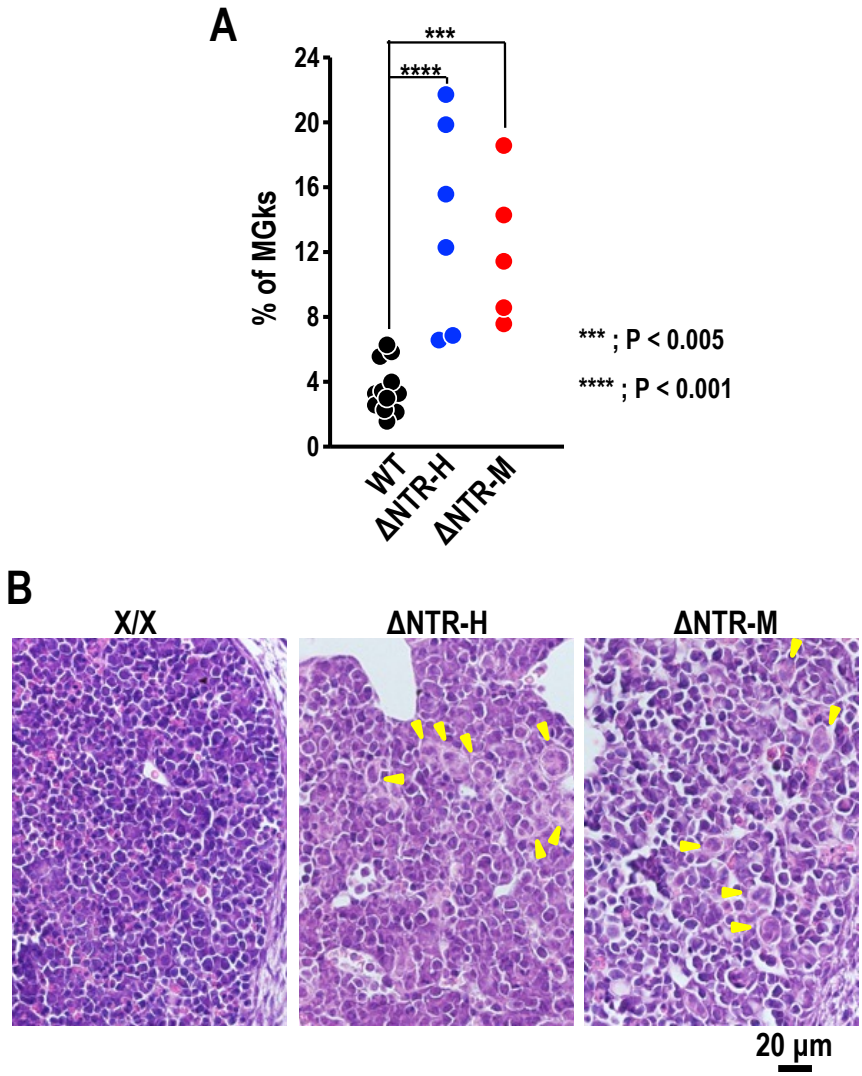

(A) Dot plot depicting the frequencies of CD41+CD61+ megakaryocytes in live cells from the fetal liver at E18.5. (B) Hematoxylin and eosin-stained sections of E12.5 ΔNTR-M and ΔNTR-H livers exhibit accumulation of large cells with a diameter exceeding 10 μm (indicated by yellow allowheads).

Supplementary Fig. 2

Histopathological analyses of liver sections of leukemic ΔNTR-M mice

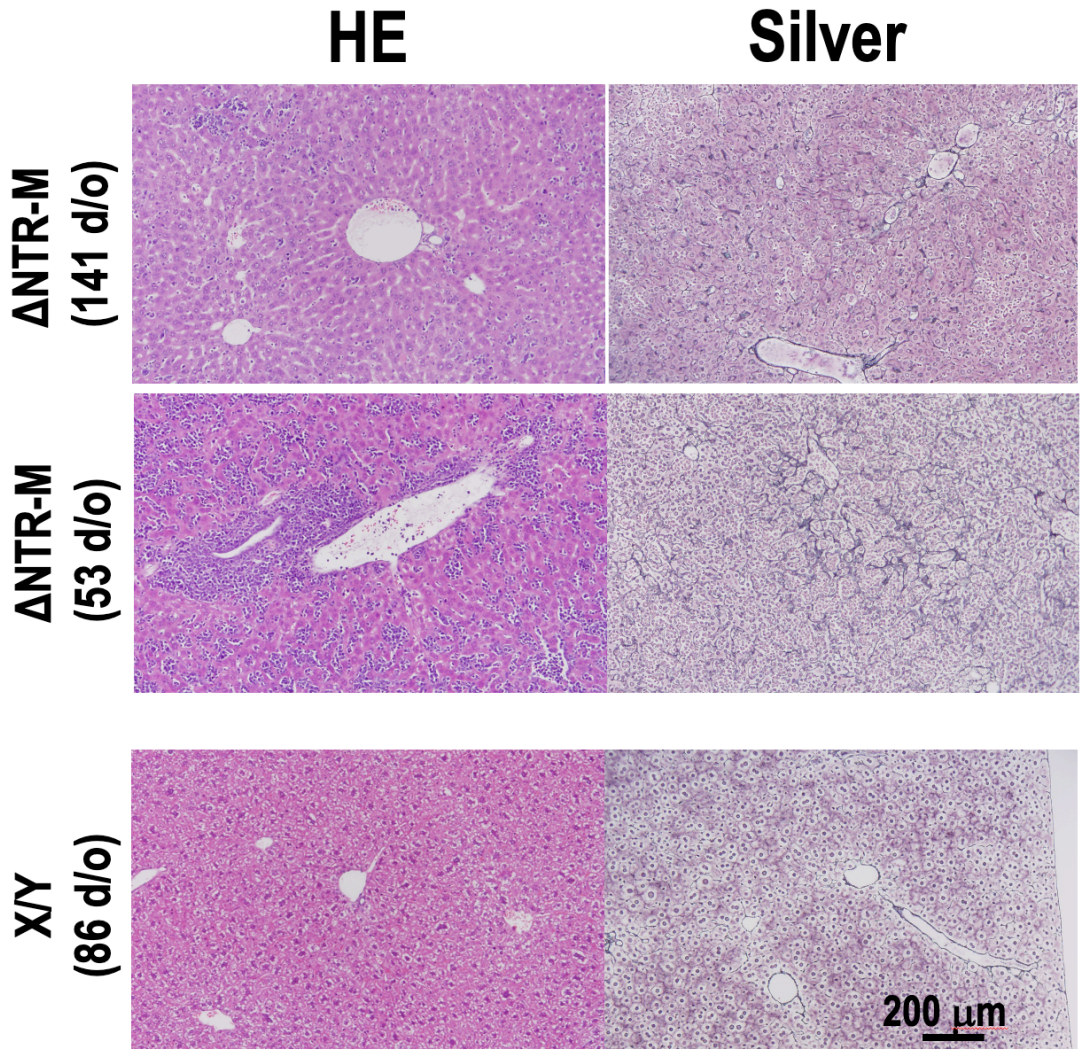

Histopathological analyses on liver sections from two ΔNTR-M mice exhibiting splenomegaly and a control wild-type mouse. Hematoxylin-Eosin staining (left panels) and silver staining (right panels) are shown. d/o: days-old.

Supplementary Fig. 3

Peripheral blood smear of a leukemic ΔNTR-M mouse

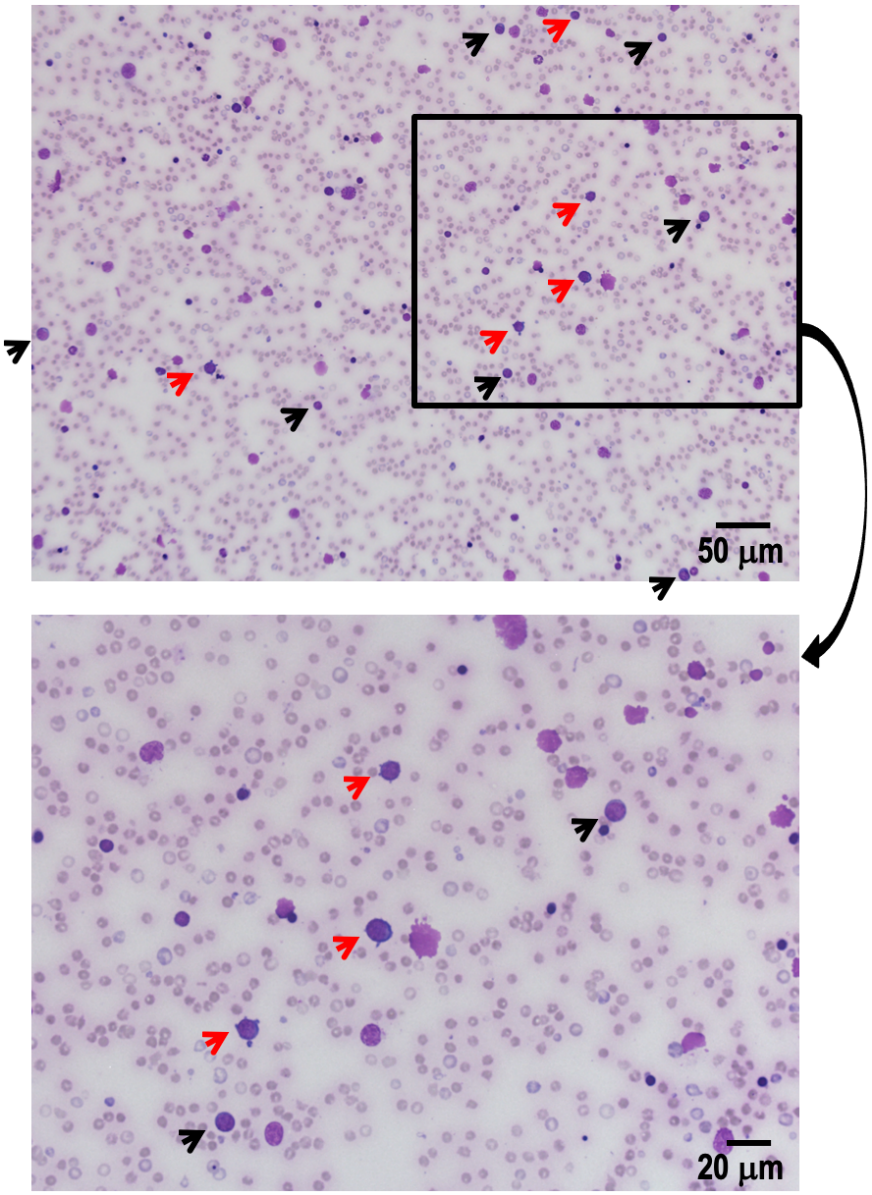

A lower magnification image (upper panel) and an enlarged image (lower panel) of the inset are presented. In these images, multiple blast cells with or without bleb formation are observed, which are indicated by red and black arrows, respectively. Additionally, numerous smudge cells are present, suggesting a hematopoietic neoplastic disease.

Supplementary Fig. 4

Leukemic cells in ΔNTR-M mouse show autonomous proliferation in recipient nude mice.

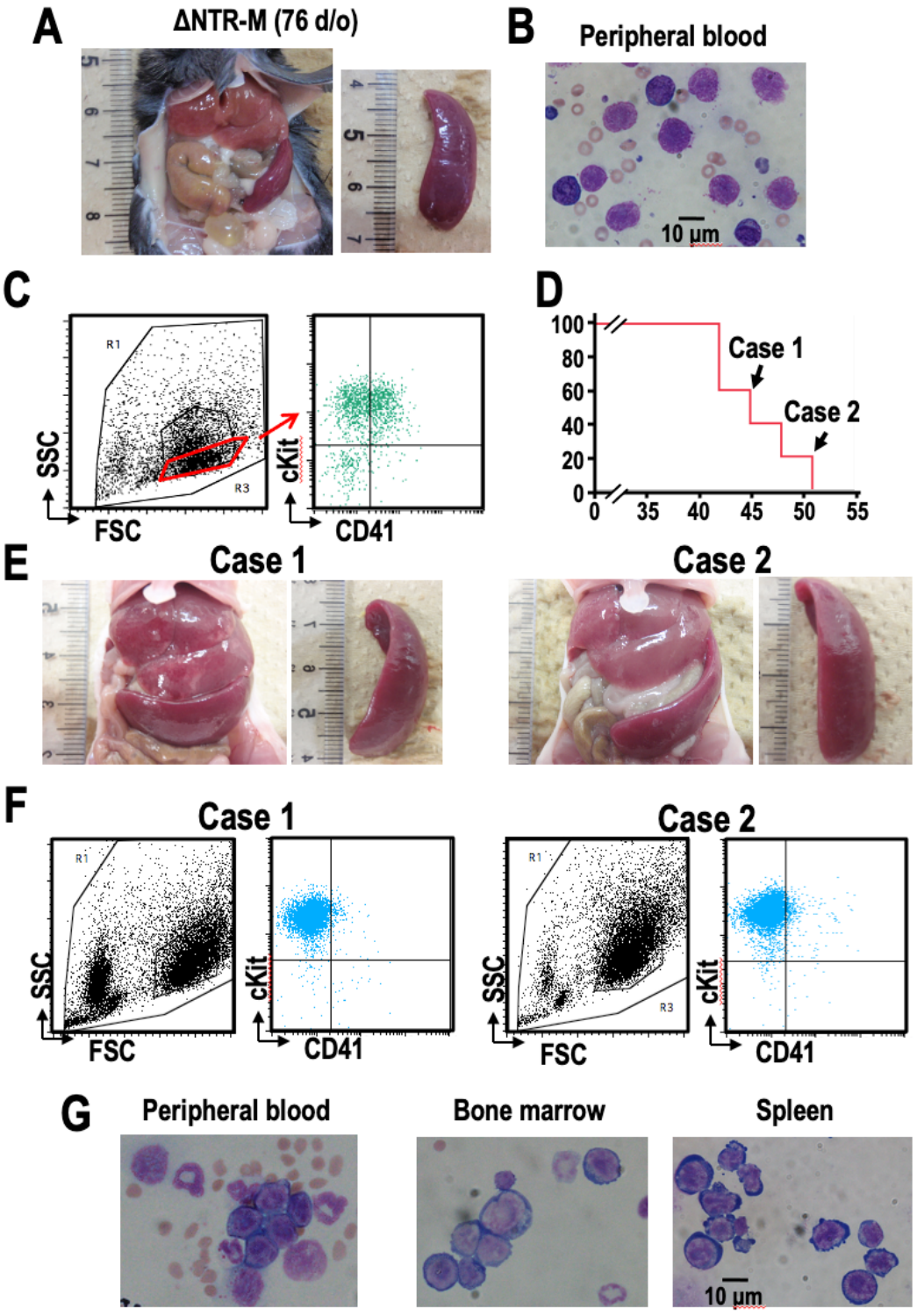

(A-C) A leukemia-developing ΔNTR-M mouse of 76 days-old (d/o) used for the transplantation analysis. Results include the macroscopic appearance (A), May-Grünwald–Giemsa staining of a peripheral blood smear (B), and flow cytometry analysis of the spleen (C). (C) Cells are visualized on FSC versus SSC (left panel), and the abnormal cells gated in the red polygon are c-Kit-positive and CD41-dull (right panel). (D) Kaplan-Meier graph depicting the outcome of five nude mice transplanted with 1 x 10^6 splenic cells from the leukemia developing ΔNTR-M mouse shown in (A). (E) Representative images from macroscopic analysis of two nude mice at 45 days (Case 1; left) and 52 days (Case 2; right) after transplantation. The spleen, liver, and body weights of mice in Case 1 are 1.97 g, 3.33 g and 22.4 g, respectively, while those in Case 2 are 0.98 g, 1.79 g and 13.5 g, respectively. (F) Flow cytometry analysis of spleen mononuclear cells from the Case 1 nude mouse (left) and that from Case 2 nude mouse (right). Cells within the abnormal fractions, marked by small black polygons in both left panels, exhibited characteristics of c-Kit^+CD41^{dull}, as seen in both right panels. (G) Blast cells in the peripheral blood smear sample (left panel) and cytospin samples from bone marrow (middle panel) and spleen (right panel). These samples were collected from the Case 1 leukemic nude mouse. Note that these leukemic cells in the nude mice exhibit similar characteristics to those observed in the donor ΔNTR-M mouse.

Supplementary Fig. 5

Integration sites of transgenes in the ΔNT-H and ΔNT-M lines.

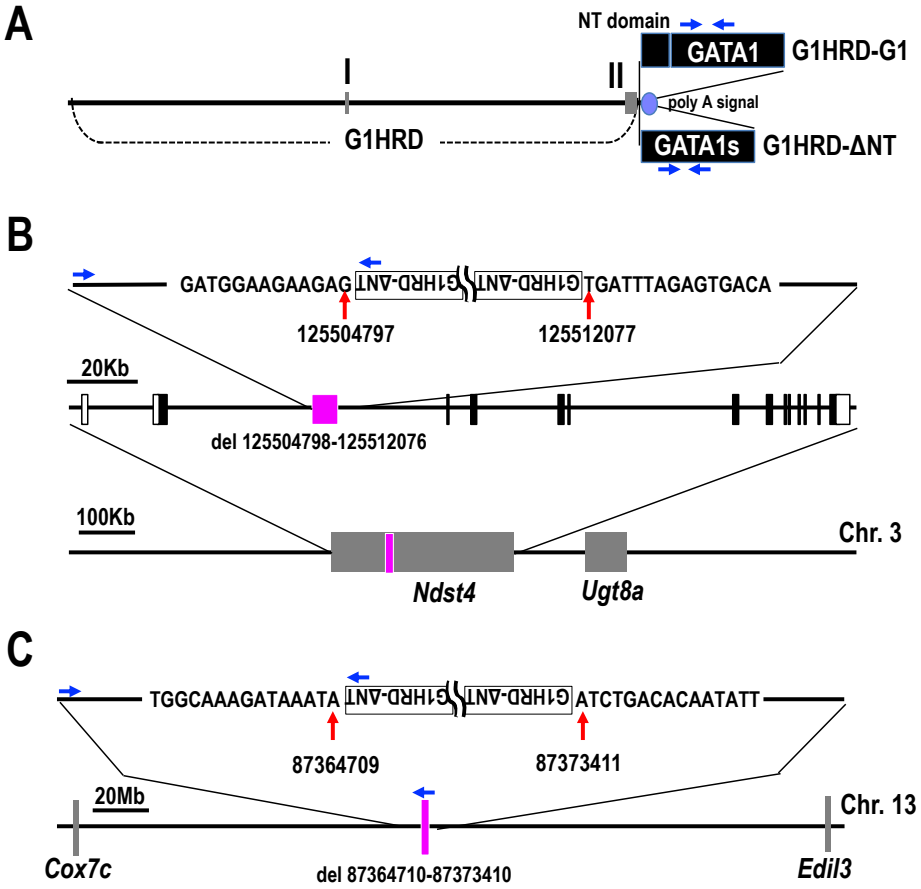

(A) Schematic representation of the G1HRD-G1 and G1HRD-ΔNT transgene constructs. Locations of primers used to identify the transgenes are indicated with blue arrows. (B, C) Schematic diagrams of the transgene-integrated sites on chromosome 3 in the ΔNT-H line of mice (B) and on chromosome 13 in the ΔNT-M line of mice (C). Notably, multiple copies (more than three [6]) of transgenes were integrated into the genomes of ΔNT-H and ΔNT-M transgenic mice. The orientations of the transgenes at both ends are depicted. Genomic position data is referenced from the GRCm38 mouse assembly. Locations of primers used to identify the transgenic and wild-type alleles are denoted with blue arrows. A reverse primer, specific for endogenous chromosome 13 allele, was designed within the sequence that was replaced by transgene in ΔNT-M line. We have determined that the transgene in the ΔNT-H mice is integrated

within the body of the *Ndst4* gene, which may represent a relatively open chromatin structure. In contrast, the transgene in ΔNT-M mice is in an intergenic region approximately 100 Mb away from the neighboring genes, suggesting a probable closed structure. We surmise that the difference in the *Gata1s* expression levels between the two transgenic mouse lines is attributable largely to the insertion site of the transgene.

Supplementary Table 1. List of mice used for experiment shown in Figure 1.

*: Mice that underwent necropsy

No.	ID	Age (day)	Genotype	Outcome
1	710	180	G1R	Surviving
2	957	180	G1R	Surviving
3	306	180	G1R	Surviving
4	308	180	G1R	Surviving
5	309	180	G1R	Surviving
6	310	180	G1R	Surviving
7	481	180	G1R	Surviving
8	487	180	G1R	Surviving
9	488	180	G1R	Surviving
10	491	180	G1R	Surviving
11	432	180	G1R	Surviving
12	183	180	G1R	Surviving
13	059	180	G1R	Surviving
14	738	180	G1R	Surviving
15	966	180	G1R	Surviving
16	298	77	ΔNTR-H	Unknown
17	441	180	ΔNTR-H	Surviving
18	496	180	ΔNTR-H	Surviving
19	501	180	ΔNTR-H	Surviving
20	433	180	ΔNTR-H	Surviving
21	434	180	ΔNTR-H	Surviving
22	435	180	ΔNTR-H	Surviving
23	436	180	ΔNTR-H	Surviving
24	350	180	ΔNTR-H	Surviving
25	222	180	ΔNTR-H	Surviving
26	187	180	ΔNTR-H	Surviving
27	724	180	ΔNTR-H	Surviving
28	727	180	ΔNTR-H	Surviving
29	188	180	ΔNTR-H	Surviving
30	191	180	ΔNTR-H	Surviving
31	195	180	ΔNTR-H	Surviving
32	448	180	ΔNTR-H	Surviving
33	351	180	ΔNTR-H	Surviving
34	619	180	ΔNTR-H	Surviving
35	029	180	ΔNTR-H	Surviving
36	030	180	ΔNTR-H	Surviving
37	484	180	ΔNTR-H	Surviving
38	779	180	ΔNTR-H	Surviving
39	223	180	ΔNTR-H	Surviving
40	083	180	ΔNTR-H	Surviving
41	670	180	ΔNTR-H	Surviving
42	672	180	ΔNTR-H	Surviving

Supplementary Table 1 (Continued)

No.		ID	Age (day)	Background	Outcome
43		673	180	ΔNTR-H	Surviving
44		674	180	ΔNTR-H	Surviving
45		031	180	ΔNTR-H	Surviving
46		061	180	ΔNTR-H	Surviving
47		005	180	ΔNTR-H	Surviving
48		808	180	ΔNTR-H	Surviving
49		470	180	ΔNTR-H	Surviving
50		482	180	ΔNTR-H	Surviving
51		337	180	ΔNTR-H	Surviving
52		653	180	ΔNTR-H	Surviving
53		174	180	ΔNTR-H	Surviving
54		176	180	ΔNTR-H	Surviving
55		165	180	ΔNTR-H	Surviving
56		166	180	ΔNTR-H	Surviving
57		167	180	ΔNTR-H	Surviving
58		198	180	ΔNTR-H	Surviving
59		104	180	ΔNTR-H	Surviving
60		101	180	ΔNTR-H	Surviving
61		102	180	ΔNTR-H	Surviving
62		194	180	ΔNTR-H	Surviving
63		957	180	ΔNTR-H	Surviving
64		491	180	ΔNTR-H	Surviving
65		329	180	ΔNTR-H	Surviving
66		782	180	ΔNTR-H	Surviving
67		964	180	ΔNTR-H	Surviving
68		684	180	ΔNTR-H	Surviving
69		017	33	ΔNTR-M	Unknown
70		199	33	ΔNTR-M	Unknown
71		044	35	ΔNTR-M	Unknown
72		414	35	ΔNTR-M	Unknown
73	*	592	38	ΔNTR-M	Leukemia
74		842	41	ΔNTR-M	Unknown
75		864	41	ΔNTR-M	Unknown
76		808	45	ΔNTR-M	Unknown
77		966	45	ΔNTR-M	Unknown
78	*	548	45	ΔNTR-M	Leukemia
79	*	723	45	ΔNTR-M	Leukemia
80	*	387	50	ΔNTR-M	Leukemia
81		728	52	ΔNTR-M	Unknown
82		757	52	ΔNTR-M	Unknown
83	*	724	53	ΔNTR-M	Leukemia
84	*	756	53	ΔNTR-M	Leukemia

Supplementary Table 1 (Continued)

No.		ID	Age (day)	Background	Outcome
85		693	60	ΔNTR-M	Unknown
86		721	60	ΔNTR-M	Unknown
87		130	67	ΔNTR-M	Unknown
88		209	67	ΔNTR-M	Unknown
89		384	88	ΔNTR-M	Unknown
90	*	071	93	ΔNTR-M	Leukemia
91	*	155	93	ΔNTR-M	Leukemia
92	*	162	120	ΔNTR-M	Leukemia
93	*	209	120	ΔNTR-M	Leukemia
94	*	337	143	ΔNTR-M	Leukemia
95	*	516	143	ΔNTR-M	Leukemia
96	*	494	146	ΔNTR-M	Leukemia
97	*	516	146	ΔNTR-M	Leukemia
98	*	663	149	ΔNTR-M	Leukemia
99	*	792	149	ΔNTR-M	Leukemia
100	*	094	150	ΔNTR-M	Leukemia
101	*	200	150	ΔNTR-M	Leukemia
102	*	396	162	ΔNTR-M	Leukemia
103		117	180	ΔNTR-M	Surviving
104		685	180	ΔNTR-M	Surviving
105		110	180	ΔNTR-M	Surviving
106		738	180	ΔNTR-M	Surviving
107		351	180	ΔNTR-M	Surviving
108		082	180	ΔNTR-MH	Surviving
109		471	180	ΔNTR-MH	Surviving
110		004	180	ΔNTR-MH	Surviving
111		009	180	ΔNTR-MH	Surviving
112		599	180	ΔNTR-MH	Surviving
113		427	180	ΔNTR-MH	Surviving
114		256	180	ΔNTR-MH	Surviving
115		470	180	ΔNTR-MH	Surviving
116		373	180	ΔNTR-MH	Surviving
117		148	180	ΔNTR-MH	Surviving
118		205	180	ΔNTR-MH	Surviving
119		088	180	ΔNTR-MH	Surviving
120	*	406	132	ΔNTR-MM	Leukemia
121		431	138	ΔNTR-MM	Unknown
122		657	180	ΔNTR-MM	Surviving
123		355	180	ΔNTR-MM	Surviving
124		071	180	ΔNTR-MM	Surviving
125		020	180	ΔNTR-MM	Surviving
126		151	180	ΔNTR-MM	Surviving

Supplementary Table 2. Primer sequences used for mouse genotyping.

		Primer sequence (5'-3')
Gata1.05 allele	F	AAGTATCCATCATGGCTGATGC
	R	TAGCCAACGCTATGTCCTGATA
Y-chromosome	F	CCTATTGCATGGACTGCAGCTTATG
	R	GACTAGACATGTCTTAACATCTGTCC
G1HRD-G1 and G1HRD-ΔNT transgene	F	AGATGAATGGTCAGAACCGG
	R	AGGCATAAGATGGCTGACAG
ΔNT-M transgene	F	GGAGACAGGATCTTCTGTAGC
	R	GGGTGATTGGGTTACCTTACTC
ΔNT-H transgene	F	CCAGAGGATAGAGAGCAATATC
	R	CAAACCACAACTAGAATGCAG
Endogenous allele at the ΔNT-M transgene integration site	F	GGAGACAGGATCTTCTGTAGC
	R	GTAGTCCTACCTGAGGGACCAG

Supplementary Table 3. Primer sequences used for Identification of transgene insertion sites.

Primer name	Primer sequence (5'-3')
G1HRD outer	GAGTACTCACATGAATCTGAGATGTC
G1HRD nested	GAGTATTCTGATCTGTCTACTGAGTGC
ΔNT3'UTR outer	GAGACAGGATCTTCTGTAGCTATGTAG
ΔNT3'UTR nested	TTTGGACAAACCACAACTAGAATGCAG

Supplementary Table 4. Primer sequences used for qPCR.

		Primer sequence (5'-3')
Gata1	F	CAGAACCGGCCTCTCATCC
	R	TAGTGCATTGGGTGCCTGC
Gapdh	F	GTCGTGGAGTCTACTGGTGTCTT
	R	GAGATGATGACCCTTTTGGC

Supplementary methods

Mice

Experimental procedures involving animals are approved by the Institutional Animal Experiment Committee of the Tohoku University. Experiments were carried out in compliance with the Regulation for Animal Experiments in Tohoku University (2015MdA-001, 2018MdA-058, 2018MdA-245, 2019MdA-289). Mice were continuously monitored for survival and were humanely euthanized upon reaching predetermined endpoints. Mice having enlarged spleen over the midline of body at necropsy were defined as those developing leukemia. Hematopoietic indices of embryos were measured by collecting blood after decapitation with surgical scissors and using a Celltac-α autohemocytometer (Nihon Koden). The *Gata1.05* allele was identified through genomic polymerase chain reaction (PCR) using a pair of primers specific to the neomycin resistance gene [6]. *Gata1* transgenes were genotyped via PCR, using a primer set designed to target the region flanking exon 4 and exon 6 of *Gata1* cDNA (Supplementary Fig. 5A). ΔNTR-MH mice were produced by crossing *Gata1.05*/X mice carrying ΔNT-H or ΔNT-M transgene with ΔNT-M or ΔNT-H transgenic male mice, respectively. Specific primer sets were used to identify ΔNT-H and ΔNT-M transgenes (Supplementary Fig. 5B, C). ΔNTR-MM mice were generated by crossing *Gata1.05*/X mice carrying the ΔNT-M transgene with ΔNT-M transgenic male mice. To distinguish ΔNTR-MM from ΔNTR-M, we used a primer set designed to recognize the endogenous allele at the site where the ΔNT-M transgene was incorporated (Supplementary Fig. 5). The primer sequences used for mouse genotyping are shown in Supplementary Table 2.

Identification of insertion sites of transgenes

Transgene insertion sites were determined using the Universal Genomic Walker Kit from

Clontech Laboratories, following the manufacturer's instruction. In brief, we amplified fragments containing genome-transgene boundary sequences from the transgenic mouse genome through nested PCR. This was achieved using transgene-specific primers in conjunction with adaptor primers provided by the manufacturer. The sequences of transgene-specific primers are shown in Supplementary Table 3. DNA fragments were purified from agarose gel and cloned into a pGEM-T vector (Promega). Subsequently, sequencing of the cloned fragments was carried out using T7 and SP6 primers, employing BigDye Terminator v3.1 Cycle Sequencing Kit and ABI PRISM 3100 Genetic Analyzer (Applied Biosystems). After excluding fragment sequences originating from the fusion of two transgenes, sequence data were analyzed through the National Center for Biotechnology Information (https://www.ncbi.nlm.nih.gov) and the DNA Data Bank of Japan (https://www.ddbj.nig.ac.jp/index-e.html) websites. Schematic illustrations depicting the genomic regions surrounding the transgenes are shown in Supplementary Fig. 5.

Flow cytometry analysis

Mononuclear cells collected from fetal liver and spleen were suspended in phosphate-buffered saline (PBS) containing 2% fetal bovine serum (FBS). Fetal liver cells were labeled with fluorescein isothiocyanate (FITC)-conjugated anti-CD41 (eBioscience) and phycoerythrin (PE)-conjugated anti-CD61 (eBioscience) antibodies. Spleen cells were labeled with FITC-conjugated anti-CD41, PE-conjugated anti-CD71 (BioLegend) and allophycocyanin conjugated anti-cKit (BD Biosciences) antibodies. After two washes with PBS, the cells were resuspended in PBS containing 2% FBS and analyzed using FACS Calibur^{TM} (Becton Dickinson Biosciences). Dead cells were excluded by propidium iodide.

RNA extraction and quantitative real-time PCR

CD41-positive cells were isolated using biotin anti-CD41 antibody (eBioscience) and

streptavidin-conjugated beads (Invitrogen). Total RNA from the CD41-positive cells was isolated using ISOGEN (NIPPON GENE). Subsequently, first-strand cDNA was synthesized using ReverTra Ace (TOYOBO). Quantitative real-time PCR was conducted utilizing the ABI PRISM 7300 sequence detector system and StepOnePlus Real-Time PCR System (Applied Biosystems) along with THUNDERBIRD SYBR qPCR Mix (TOYOBO). The data were normalized to the *Gapdh* mRNA level. The primer sequences employed for the expression analysis are provided in Supplementary Table 4.

Proplatelet formation assay

Mononuclear cells were suspended in CATCH-medium (doi: 10.1083/jcb.69.1.159) and overlaid on a discontinuous BSA gradient (2%/3%/4%/16% in CATCH-medium). After 1 hour, the upper half of the gradient was combined and washed with CATCH-medium. Subsequently, cells were resuspended in 2-ml IMDM-medium containing Nutridoma-SP (Behringer-Mannheim). After a 24 hour-incubation at 37ºC, the frequencies of megakaryocytes forming proplatelets were assessed.

Histological and cytological analysis and microscope

Cytospin samples of bone marrow and spleen cells were prepared using a cytocentrifuge (Thermo Fisher Scientific). Peripheral blood smear samples and cytospin samples were stained with May–Grünwald staining solution (Merck) and Giemsa staining solution (Merck). Formalin-fixed tissue sections were stained with Hematoxylin-eosin and Watanabe's silver impregnation method. Images of mice were monitored by μTOUGH-8000 (Olympus). Images of tissues were captured using a BX51 microscope (Olympus) and images of cells expressing GFP were captured using MZFLIII stereomicroscopes (Leica), and were photographed using a DP73 CCD-camera (Olympus).

Statistical analysis

All statistical analyses were done using JMP software (SAS Institute Inc.). Survival rates were analyzed using the Kaplan-Meier method. The data was analyzed using a Mann-Whitney U test. Mortality of various mouse groups were compared using the Log-rank test and Generalized Wilcoxson test.